ASTROPHYSICAL SEARCHES FOR EXOTIC PHENOMENA IN ULTRAHIGH ENERGY NEUTRINO–NUCLEON SCATTERING[*]

D.A. MORRIS[†]

University of California, Los Angeles, 405 Hilgard Ave.
Los Angeles, CA 90024, U.S.A.

and

A. RINGWALD[‡]

DESY, Notkestrasse 85
D–22603 Hamburg, Germany

ABSTRACT

We investigate the potential of near–future neutrino telescopes like NESTOR for searches for exotic processes in ultrahigh energy neutrino–quark scattering. We consider signatures such as muon bundles and/or contained cascades from the nonperturbative production of multiple weak gauge bosons in the Standard Model, compositeness and leptoquark production.

---

1. Introduction

The introduction of neutrino telescopes such as AMANDA[1], Baikal NT–200[2], DUMAND[3], and NESTOR[4] will begin a new era in astronomy. In this talk we report on how these detectors might also enlarge our knowledge of particle physics. In particular, we wish to explore the sensitivity of NESTOR to exotic processes in ultrahigh energy neutrino–quark scattering at center of mass energies in the multi–TeV region. Such energies will only become accessible to terrestrial accelerators after the commissioning of CERN's proposed Large Hadron Collider (LHC).

Compared to the sophistication of compact, accelerator–based detectors, water Cherenkov detectors such as NESTOR concentrate on relatively specific characteristics of individual events. To compensate for this limitation, we will restrict our discussion to three examples of exotic phenomena with particularly striking signatures: 1) the multiple production of weak gauge bosons (W,Z) due to nonperturbative features of the standard electroweak theory (multi-W processes), ii) multiple production of quarks and leptons due to compositeness of quarks and leptons, and iii) the formation and decay of leptoquarks in the neutrino–quark subprocess.

To be quantitative, we will adopt a phenomenological approach to investigate the existence of exotic processes. We will parametrize the anticipated features of new phenomena and then ask what region of parameter space is accessible to near–future experiments. Our presentation will proceed as follows. In section 2 we review the phenomenology expected if nonperturbative multiple weak gauge boson production exists. Since this phenomena exists entirely within the framework of the Standard Model, we devote considerable attention to it. As our discussion of multi–W phenomena progresses, we introduce neutrino fluxes and describe the geometry of the stage–2 NESTOR array which we use in our subsequent calculations. In sections 3 and 4 we discuss compositeness and leptoquarks respectively.

2. Neutrino–Initiated Multi–W(Z) Production

2.1. Nonperturbative Multi–W(Z) Production

A few years ago it was realized[5−8] that, even within the context of a weakly coupled Standard Model, leading–order perturbative calculations of the inelastic

scattering of quarks and leptons involving the production of $\gtrsim \mathcal{O}(\alpha_W^{-1}) \simeq 30$ weak gauge bosons result in an explosive (and unitarity violating) growth of the associated parton-parton cross section above center of mass energies $\gtrsim \mathcal{O}(\alpha_W^{-1} M_W) \simeq 2.4$ TeV. It was found that, to leading–order in α_W, amplitudes for the production of n_W W and Z bosons (*e.g.*, in neutrino–quark collisions) exhibit a factorial growth in n_W. This happens both for baryon and lepton number (B+L) conserving amplitudes[7−9],

$$\mathcal{A}_{\text{lead. ord.}}^{\text{B+L cons.}}(\nu + q \to \ell + q + n_W \; W(Z)) \propto n_W! \; \alpha_W^{n_W/2} \left(\frac{n_W}{\sqrt{\hat{s}}}\right)^{n_W}, \tag{1}$$

as well as for anomalous B+L violating amplitudes[5,6],

$$\mathcal{A}_{\text{lead. ord.}}^{\text{B+L viol.}}(\nu + q \to 8\overline{q} + 2\overline{\ell} + n_W \; W(Z)) \propto$$
$$n_W! \; \alpha_W^{n_W/2} \left(\frac{\sqrt{\hat{s}}}{n_W m_W}\right)^{n_W} \frac{e^{-2\pi/\alpha_W}}{m_W^{n_W}} \; . \tag{2}$$

Perturbation theory applied to large order processes (*e.g.*, like the production of $\mathcal{O}(\alpha_W^{-1})$ weak bosons) breaks down somewhere in the multi–TeV range. It is presently an open theoretical question whether large–order weak interactions become strong at this energy scale (in the sense of having observable cross sections) or whether they remain unobservably small at all energies. The answer almost certainly lies beyond the realm of conventional perturbative techniques (see Ref. 10 for an overview). A quantitative consideration of experimental constraints on multi–W production is clearly desirable. In this section we report on our recent investigations of this question[11,12] (see also Refs. 13–15).

2.2. Parametrization of Multi–W(Z) Production

In the absence of a reliable first–principles calculation of multi–W production, we parametrize the quark–quark or neutrino–quark cross section for multi–W production by

$$\hat{\sigma}_{\text{multi−W}} = \hat{\sigma}_0 \; \Theta(\sqrt{\hat{s}} - \sqrt{\hat{s}_0}). \tag{3}$$

This two–parameter working hypothesis frees us from specifying an underlying (and most likely nonperturbative) mechanism for multi–W production. According to our

3

parameterization the parton-parton cross section for multi-W production turns on with a strength $\hat{\sigma}_0$ above a parton-parton center of mass threshold energy $\sqrt{\hat{s}_0}$. By convoluting the subprocess cross section of Eq. (3) with the appropriate quark distribution functions, one obtains the multi–W production cross sections appropriate for nucleons. For definiteness, we will assume throughout this talk that $\hat{\sigma}_0$ refers to the production of exactly 30 W bosons; allowing for the production of variable numbers of W's (and Z's and possibly prompt photons) is straightforward but is an unnecessary complication at the level of our investigation.

An optimistic range of parameters to consider might encompass

$$
\frac{m_W}{\alpha_W} \simeq 2.4 \text{ TeV} \;\; \leq \;\; \sqrt{\hat{s}_0} \;\; \leq \;\; 40 \text{ TeV},
$$

$$
\frac{\alpha_W^2}{m_W^2} \simeq 100 \text{ pb} \;\; \leq \;\; \hat{\sigma}_0 \;\; \leq \;\; \sigma_{\text{inel}}^{pp} \times \left(\frac{1 \text{ GeV}}{m_W} \right)^2 \simeq 10 \text{ } \mu\text{b}.
$$

(4)

The lower limit of $\sqrt{\hat{s}_0}$ is suggested by the energy scale at which perturbation theory becomes unreliable[7−9] whereas the upper range is of the order of the sphaleron mass[16], the characteristic scale of anomalous electroweak B+L violation. Unitarity arguments suggest[17] that the cross section for nonperturbative multi–W(Z) production is always exponentially suppressed, $\hat{\sigma}_0 \propto \exp(-c/\alpha_W)$, with $0 \;\; < \;\; c \lesssim 2\pi$. However, this does not exclude the possibility of a small coefficient $(c \ll 1)$ such that an observable cross section results[18]. The lower limit of $\hat{\sigma}_0$ is characteristic of a geometrical "weak" cross section and the upper limit range is a geometrical "strong" cross section suggested by analogies between the weak SU(2) gauge sector and the color SU(3) gauge sector[19].

The simultaneous production of $\mathcal{O}(30)$ W bosons at future hadron colliders such as the proposed LHC would lead to spectacular signatures[20,21]. Since approximately 20 charged hadrons (mainly $\pi^{\pm}$'s) arise from hadronic W decays one could typically expect 400 $\pi^{\pm}$'s in one multi–W event accompanied by $\simeq 400$ photons from the decay of $\simeq 200$ π^0's. The charged hadrons would have a minimum average transverse momentum of order $p_T^{\pi} \geq \mathcal{O}(m_W/30) \simeq (2-3)$ GeV if the W bosons are produced without transverse momentum. Similarly, one could expect $\simeq 5$ prompt muons ($\simeq 3$ from W decays and $\simeq 2$ from c, b, or τ decay) carrying a minimum average transverse momentum of $p_T^{\mu} \geq \mathcal{O}(m_W/2) \simeq 40$ GeV. Analogous situations hold for other prompt leptons such as $e^{\pm}, \nu$ etc. No conventional reactions in the

Standard Model are backgrounds to multi–W processes[21].

Figure 1 shows the regions in $\sqrt{\hat{s}_0} - \hat{\sigma}_0$ space accessible to the LHC. The contours give the number of multi-W reactions occurring during 10^7 s of operation (assuming 100% detection efficiency). These contours may be used as a benchmark to evaluate the effectiveness of various cosmic ray physics experiments for constraining multi–W phenomena[12].
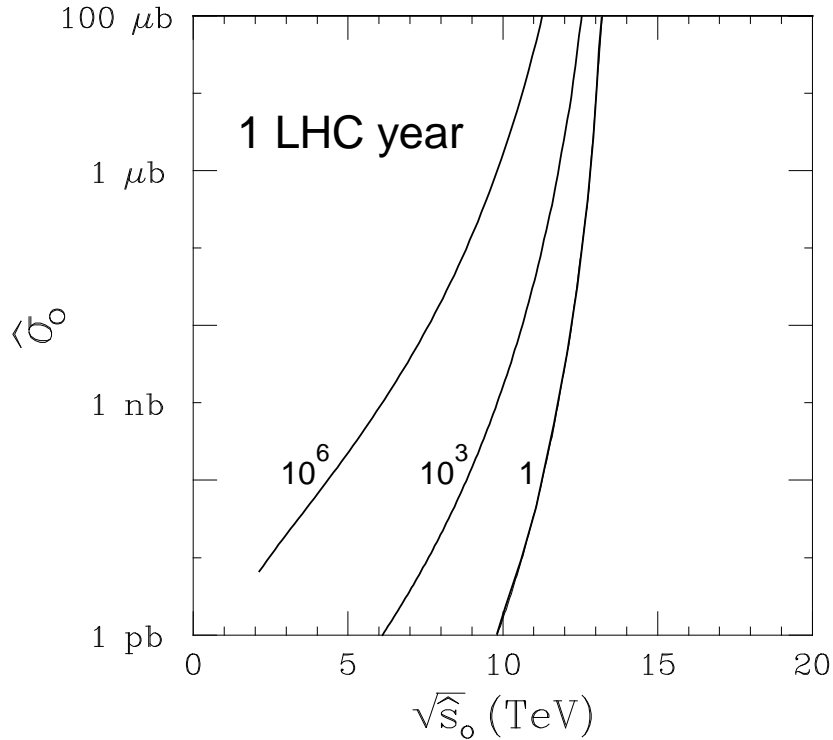

Fig. 1. Contours corresponding to $1, 10^3, 10^6$ multi–W events in one year (10^7 s) of operation for the LHC ($\sqrt{s_{pp}} = 14$ TeV; luminosity 10^{34} cm^{-2}s^{-1}).

2.3. NESTOR's Multi–W(Z) Discovery Potential

Until the proposed LHC becomes available, cosmic rays provide our only access to parton–parton center of mass energies in the multi–TeV range. However, having energetic cosmic rays is not sufficient; due to small event rates, it is only practical to search for phenomena which have spectacular low–background signatures. In this section we review the appeal of neutrino–induced phenomena and discuss NESTOR's potential for investigating multi–W processes.

While there is an ample flux of multi–PeV cosmic protons bombarding the Earth, it appears hopeless that one could exploit this flux to search for multi–W phenomena[12]. The source of the difficulty is that, due to a generic QCD–dominated $\mathcal{O}(100 \text{ mb})$ proton–proton total cross section, only a small fraction ($\sigma^{pp}_{\text{multi–W}}/\sigma^{pp}_{\text{total}}$) of the incident cosmic proton flux is available for multi–W processes. The proton flux attenuation due to large competing generic QCD cross sections is so severe that even for the most optimistic values of $\sqrt{\hat{s}_0}$ and $\hat{\sigma}_0$ only 1–100 extensive air showers of multi–W origin would be incident on 100 km^2 in one year (see Ref. 12 for details). Moreover, the characteristics of these 1–100 multi–W showers would not be sufficiently distinctive to avoid confusion with fluctuations in the background of generic air showers. Given these prospects, one abandons hope of exploiting the cosmic proton flux for uncovering multi–W processes.

Cosmic neutrinos, on the other hand, suggest an attractive alternative. Since conventional charged current neutrino–nucleon cross sections are anticipated to be of $\mathcal{O}(1-10 \text{ nb})$ in the energy range in which we are interested, neutrino flux attenuation due to generic processes is not an issue unless we wish to search for phenomena with cross sections orders of magnitude smaller. Furthermore, we gain the added discrimination that neutrino–initiated phenomena typically occur deep in the atmosphere or inside the Earth due to a small total neutrino–nucleon cross section (which conceivably could be dominated by new physics).

There is, however, a drawback to using ultrahigh energy neutrinos as a probe for new physics: we do not know their flux. Though atmospheric neutrinos (*i.e.,* neutrinos produced in hadronic showers in the atmosphere) are a guaranteed source of neutrinos, their flux in the PeV region is anticipated to be negligible[22] (see Fig. 2). More promising are recent predictions of a sizeable flux of PeV neutrinos from active galactic nuclei (AGN)[23−26]. For definiteness, we consider the (revised) Stecker *et al.*[23] AGN neutrino flux of Fig. 2. AGN neutrino fluxes calculated under different assumptions in Refs. 24, 25 generally agree with Ref. 23 above .1 PeV, which is the energy range we are interested in. In this sense our use of the Stecker *et al.* flux is intended to be representative of a large class of AGN flux models. In Ref. 12 we have checked that, within the parameter ranges of Eq. (4), large neutrino cross sections for multi–W production are consistent with proposed AGN flux models.

In addition to the proposed AGN neutrino fluxes, we will also consider the

possibility of exploiting neutrinos produced when ultrahigh energy protons inelastically scatter off the cosmic microwave background radiation[27] (CBR) in processes such as $\gamma p \to \Delta \to n\pi^+$ where the produced pion subsequently decays[28–30]. As shown in Fig. 2, such processes may provide the dominant component of the neutrino flux at energies beyond $\simeq 1$ EeV. The CBR neutrino fluxes shown in Fig. 2 are taken from Ref. 23.
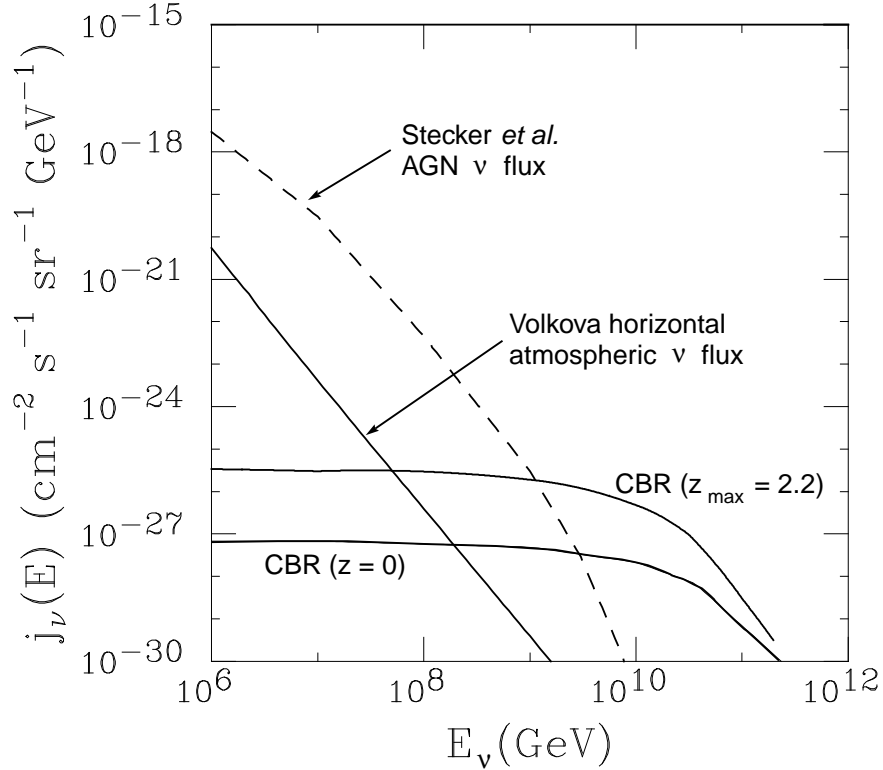

Fig. 2. Differential flux of neutrinos used in text. The horizontal flux of atmospheric neutrinos is taken from Volkova[22]. The diffuse flux of neutrinos from active galactic nuclei (AGN) and the neutrino flux due to inelastic scattering of cosmic ray protons off the cosmic microwave background radiation (CBR) are from Stecker *et al.*[23]. The above fluxes are summed over all neutrino species.

NESTOR may be used to search for multi–W phenomena in at least two ways: 1) through the detection of muon bundles which originate from the prompt decays of many W bosons produced far $(\gtrsim \mathcal{O}(1 \text{ km}))$ from the detector[12–15] and 2) through the detection of the cascade produced by a nearby $(\lesssim \mathcal{O}(1 \text{ km}))$ neutrino–nucleon multi–W process. For definiteness, we will restrict our considerations to the

stage–2 NESTOR array depicted in Fig. 3. A stage–1 NESTOR array consisting of a single tower (as in Fig. 3c) is comparable to a fully constructed DUMAND array whose response to multi–W phenomena is discussed in Ref. 12.
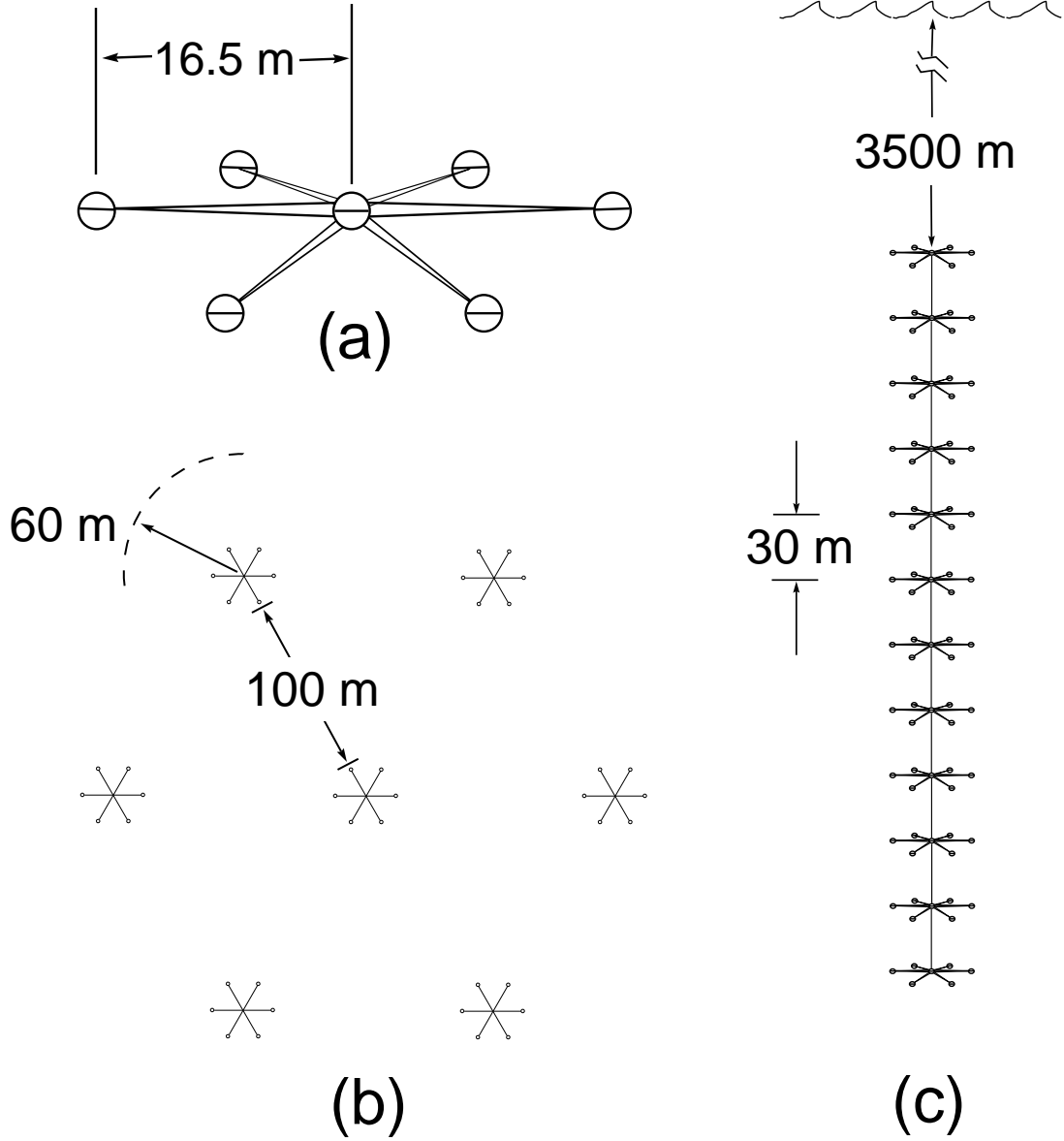

Fig. 3. Parameters of the stage–2 NESTOR array assumed in this paper. (a) Hexagonal frame of 16.5 m radius supports up– and down–looking phototubes. (b) Top view of stage–2 array composed of seven towers. For simulations we assume each tower efficiently reconstructs muons within 60 m radius (appropriate for 10 TeV muons). (c) A single tower is made up of twelve hexagonal frames. The average sea depth of a tower is 3665 m (= 3500 m + 330/2 m).

Figure 4a shows the expected number of multi–W events detected through muon bundles in 10^7 s for a stage–2 NESTOR array assuming the AGN neutrino flux of Stecker *et al.* Details of the calculation may be found in Refs. 12,13. As a simplifying approximation, we assume that the stage–2 NESTOR array reconstructs muon trajectories inside a cylindrical fiducial volume of radius 193 m (= 60 m + 100 m + 2 × 16.5 m from Figs. 3a,b) and height of 330 m (from Fig. 3c). The muon bundles consist of 2–3 muons originating from the prompt decays of 30 W bosons. Also shown in Fig. 4a are contours of the average zenith angle cosine corresponding to the arrival direction of the muon bundles.
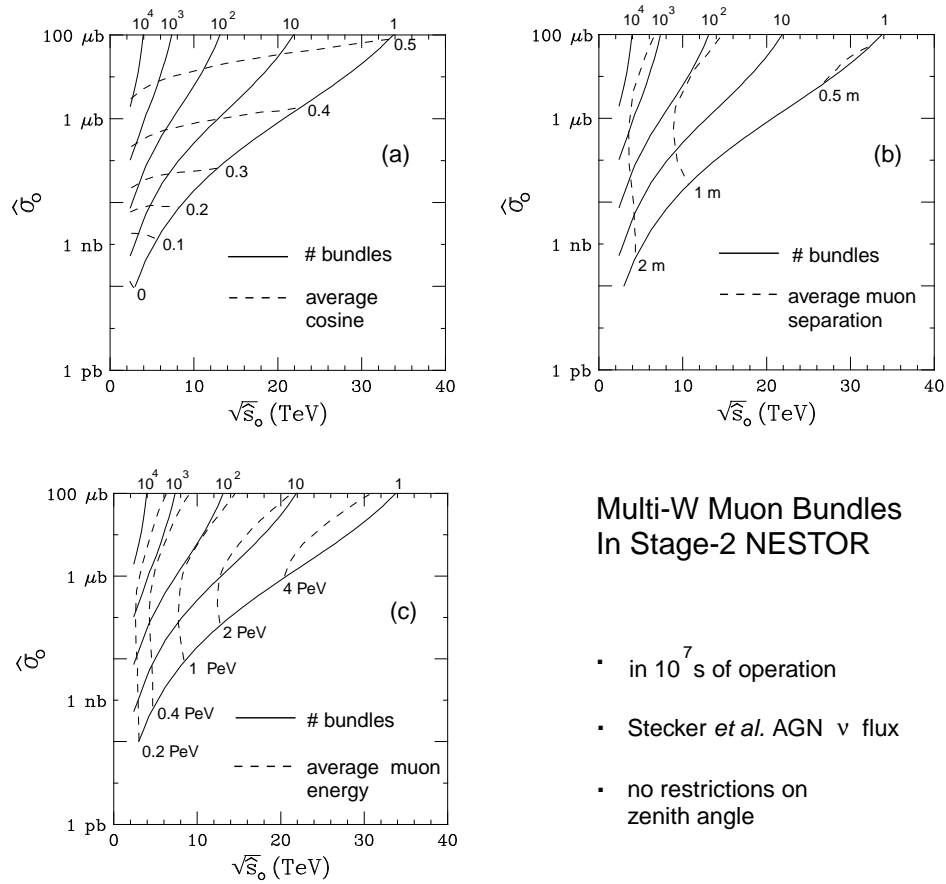

Fig. 4. a) Contours for the number of muon bundles from neutrino–initiated multi–W processes passing through a stage–2 NESTOR fiducial volume in 10^7 s assuming the Stecker *et al.* AGN neutrino flux. Solid contours give the number of events (labels appear along top of graph) while dashed contours indicate the average zenith angle cosine of the muon bundle arrival direction. b) Solid: same as in (a); dashed: average inter-muon separation within a muon bundle. c) Solid: same as in (a); dashed: average muon energy as muons pass through fiducial volume.

9

Figure 4b shows the average inter–muon separation within a muon bundle of multi–W origin. Inter–muon separations of less than a few meters call into question the ability of a water Cherenkov detector to recognize the multi–muon nature of such events. To our knowledge this experimental issue has not been addressed in any detail. Figure 4c includes contours of the average muon energy as the muons pass through the detector. Muon energies in the range of 10–1000 TeV ensure their detection. The large muon energies (and small inter–muon separations) of Figs. 4b,c reflect the kinematics of the enormous cosmic neutrino energy required to initiate a multi–W process characterized by a multi–TeV parton–parton threshold.

We emphasize that the contours in Fig. 4 only chronicle the *average* value of each observable at each point in $\sqrt{\hat{s}_0} - \hat{\sigma}_0$ space. For example, Fig. 5 shows the distributions of zenith cosine, intermuon separation and muon energy for the parameter choice ($\sqrt{\hat{s}_0} = 4$ TeV, $\hat{\sigma}_0 = 10$ nb) — the averages of these distributions correspond to single points in Figs. 4a,b,c respectively.
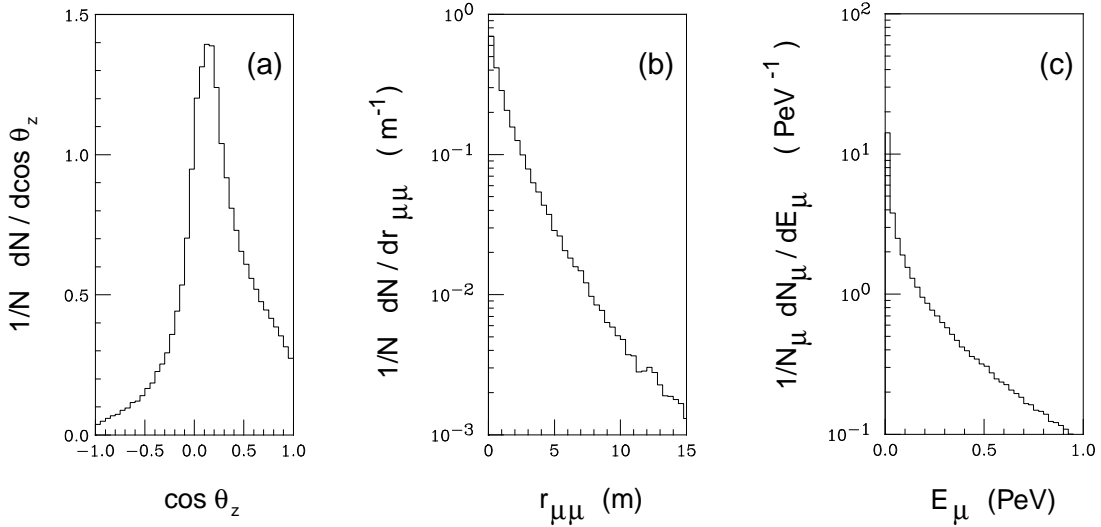

Fig. 5. Distributions corresponding to muon bundles from neutrino–initiated multi–W processes (with fixed $\sqrt{\hat{s}_0} = 4$ TeV, $\hat{\sigma}_0 = 10$ nb) passing through a NESTOR stage–2 fiducial volume assuming the Stecker *et al.* AGN neutrino flux. (a) Distribution of muon bundle arrival direction ($\langle\cos\theta_z\rangle = .21$). (b) Distribution of the average lateral separation between muons within a bundle. Assuming the production of exactly 3 muons from the prompt decays of 30 W bosons, approximately 90%(10%) of the bundles making it to the detector consist of 3(2) muons ($\langle r_{\mu\mu}\rangle = 2.0$ m). (c) Distribution of individual muon energy as muon passes through fiducial volume ($\langle E_\mu\rangle = .33$ PeV). Distributions shown in (a),(b) and (c) are normalized to unity. A total of 22 muon bundles pass through the fiducial volume in 10^7 s.

To eliminate the possibility of a muon–bundle background due to atmospheric muons produced in generic hadronic air showers, one can restrict a search to muon bundles arriving only from zenith angles with $\theta_z > 80^o$. By looking towards large zenith angles we are assured that muons reaching the detector are produced inside the Earth and hence are not due to generic interactions in the atmosphere. Figure 6 illustrates the potential of a stage–2 NESTOR which looks only at muon bundles with $\theta_z > 80^o$.
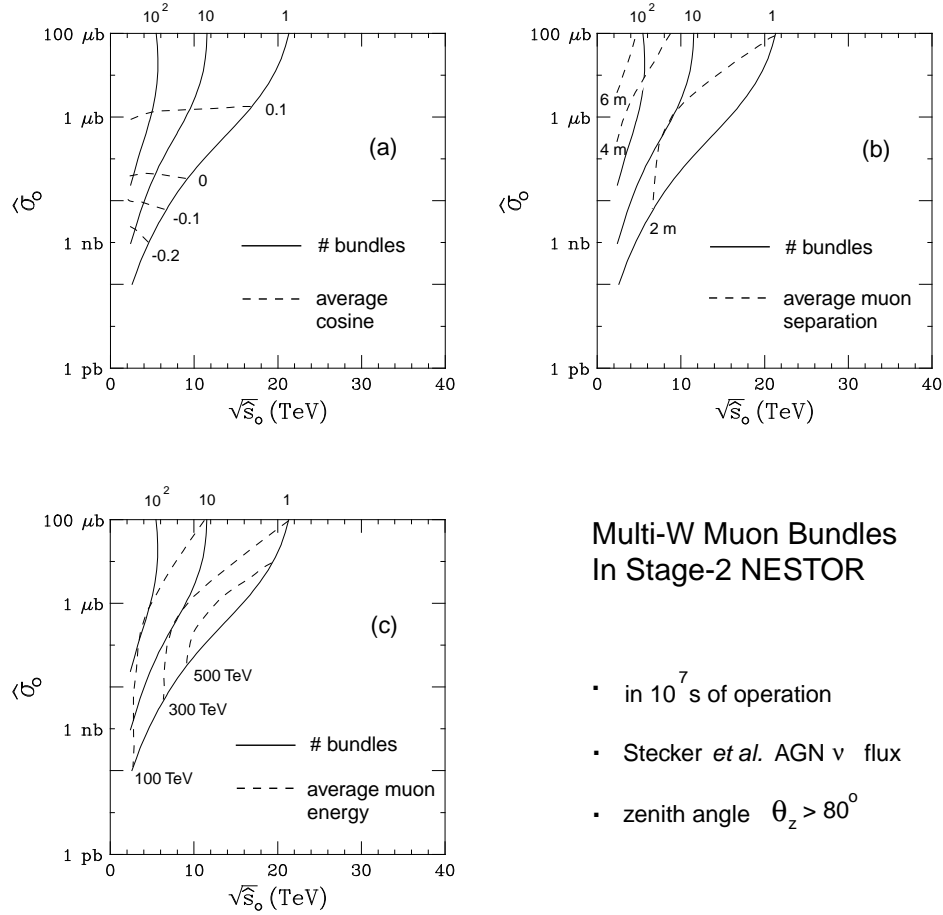

Fig. 6. a) Contours for the number of muon bundles arriving with zenith angle $\theta_z > 80^o$ from neutrino–initiated multi–W processes passing through a stage-2 NESTOR fiducial volume in 10^7 s assuming the Stecker $et\ al.$ AGN neutrino flux. Solid contours give the number of events while dashed contours indicate the average zenith angle cosine of the muon bundle arrival direction. b) Solid: same as in (a); dashed: average inter-muon separation within a muon bundle. c) Solid: same as in (a); dashed: average muon energy as muons pass through fiducial volume.

11

If, in addition to AGN neutrinos, we include a flux component due to neutrino production off the cosmic microwave background, we obtain the discovery contours for near–horizontal muon bundles shown in Fig. 7. While it appears that including a CBR neutrino flux component can, in principle, greatly extend the range of $\sqrt{\hat{s}_0}$ probed, we must point out the sensitivity to the flux model assumed. For example, had we used the minimum CBR neutrino flux (labelled $z = 0$ in Fig. 2) the contour corresponding to one detected event in Fig. 7, which extends up to $\sqrt{\hat{s}_0} \simeq 50$ TeV, would collapse back to its position shown in Fig. 6.
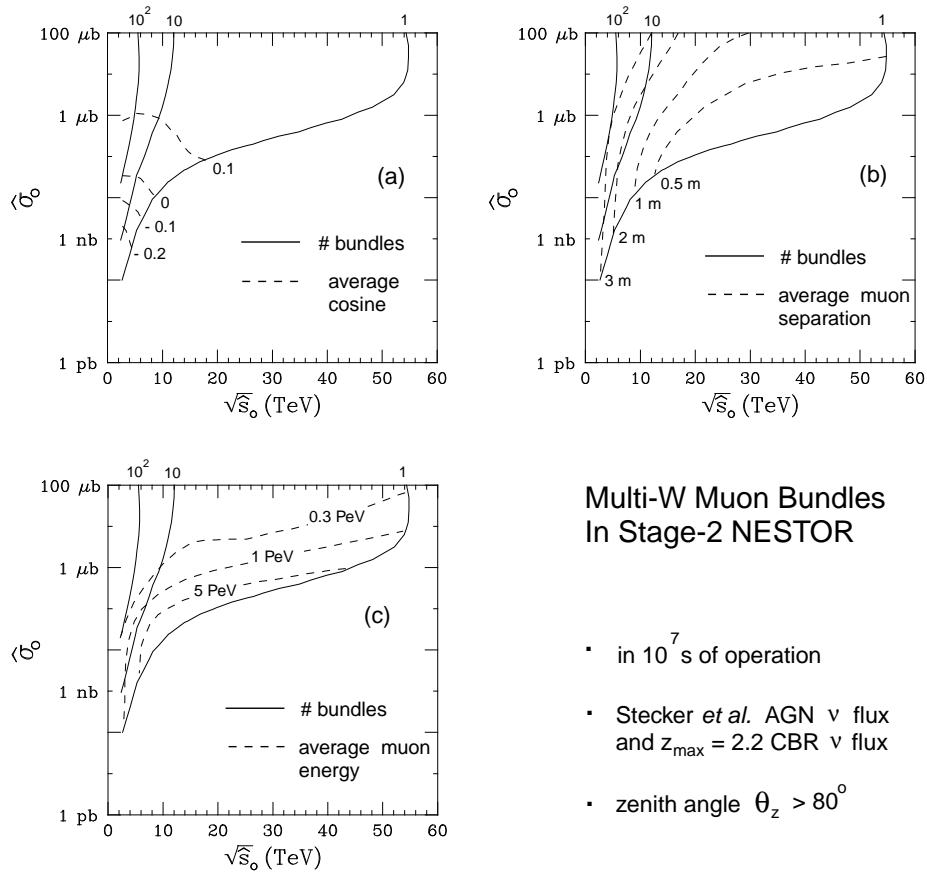

Multi-W Muon Bundles
In Stage-2 NESTOR

- in 10^7 s of operation

- Stecker *et al.* AGN ν flux and $z_{max} = 2.2$ CBR ν flux

- zenith angle $\theta_z > 80^o$

Fig. 7. a) Contours for the number of muon bundles arriving with zenith angle $\theta_z > 80^o$ from neutrino–initiated multi–W processes passing through a stage–2 NESTOR fiducial volume in 10^7 s assuming the Stecker *et al.* AGN neutrino flux and the CBR neutrino flux component labelled $z_{max} = 2.2$ in Fig. 2. Solid contours give the number of events while dashed contours indicate the average zenith angle cosine of the muon bundle arrival direction. b) Solid: same as in (a); dashed: average inter–muon separation within a muon bundle. c) Solid: same as in (a); dashed: average muon energy as muons pass through fiducial volume.

Turning now to the detection of underwater cascades, the effective volume of stage–2 NESTOR can be much larger than the volume appropriate for detecting the Cherenkov light from throughgoing muons; we will assume a sensitive volume of 1 km^3, appropriate for multi–PeV cascades, for "contained" multi–W phenomena. Figure 8 shows the discovery contours for contained multi–W phenomena assuming the Stecker *et al.* AGN neutrino flux and a CBR neutrino flux component (labelled $z_{max} = 2.2$ in Fig. 2). The contour for one detected event in Fig. 8 is subject to the same sensitivity to the CBR flux model as discussed in the previous paragraph. The contours for the average energy of a multi-W cascade assume that 20% of the initiating neutrino's energy is given to prompt neutrinos and muons (through W decay) and is not observed.
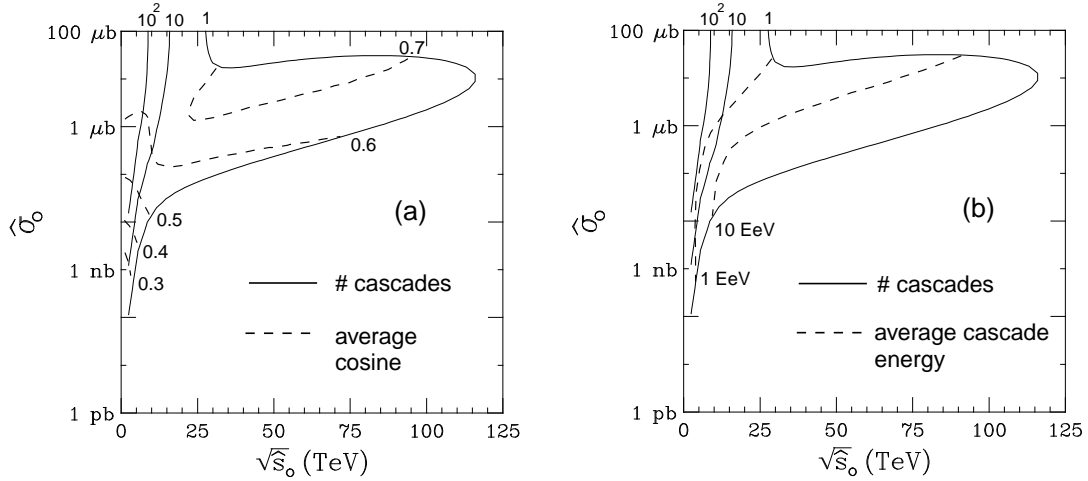

Fig. 8. a) Contours for the number neutrino–initiated multi–W processes contained in a 1 km^3 fiducial volume at stage–2 NESTOR in 10^7 s assuming the Stecker *et al.* AGN neutrino flux and the CBR neutrino flux component labelled $z_{max} = 2.2$ in Fig. 2. Solid contours give the number of events while dashed contours indicate the average zenith angle cosine of the original neutrino. b) Solid: same as in (a); dashed: average energy of the contained cascade.

Unlike the search for near–horizontal muon bundles, contained multi–W phenomena may have backgrounds due to generic charged current processes. We estimate these backgrounds as follows. At the energies we are interested in, the lepton ℓ in a generic charged current process $\nu N \to \ell + X$ carries away an average of 80% of the incident neutrino energy[31]. Hence if ℓ is a muon, only about 20% of the incident neutrino energy can appear in the contained cascade. Treating generic ν_μ and $\bar{\nu}_\mu$

13

cascades in this manner, we consider the background to contained multi–W production to be any contained cascade with energy greater than $E_{\text{thresh}}/10$ where E_{thresh} is the threshold energy required of a neutrino to initiate a multi–W process. We include background cascades with energies ten times less than E_{thresh} in an attempt to account for the limited energy resolution of neutrino telescopes. Figure 9 compares the rate, energy and direction of contained cascades due to generic charged current interactions and multi–W processes.
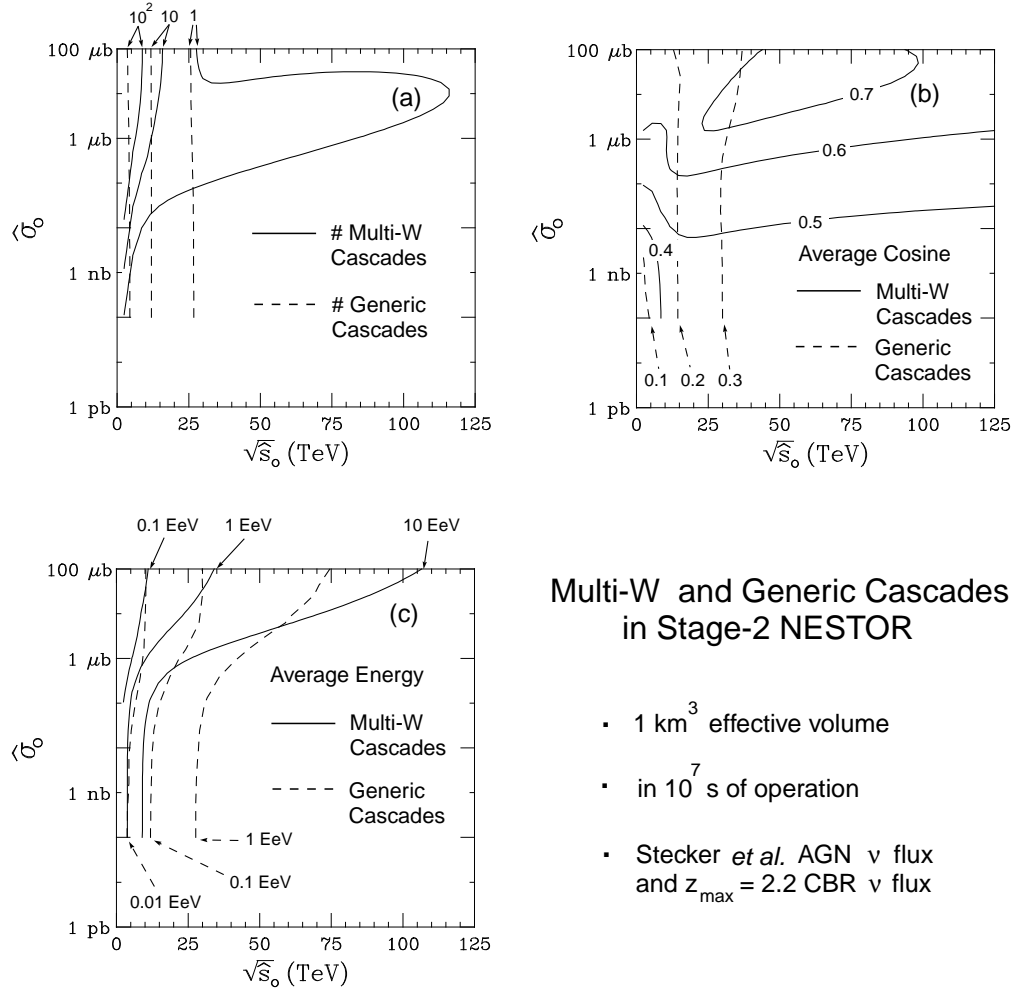

Fig. 9. Comparison of a) rate b) direction and c) energy of contained cascades due to multi–W processes (solid) and generic charged current interactions (dashed). Contours correspond to neutrino–initiated cascades in a 1 km^3 fiducial volume at stage–2 NESTOR in 10^7 s assuming the Stecker *et al.* AGN neutrino flux and the CBR neutrino flux component labelled $z_{\text{max}} = 2.2$ in Fig. 2. Multi–W contours are same as in Fig. 8. Criteria for background cascades are described in text.

14

An additional process which will lead to spectacular contained cascades is due to resonant W production through the Glashow process $\overline{\nu}_e + e^- \rightarrow W^- \rightarrow$ hadrons. Under the same detector and flux conditions as in Fig. 9, we find that there should be approximately 9 contained resonant interactions in 10^7 s at stage–2 NESTOR of which 6 would involve hadronic decays of the W boson. These 6 cascades would have average energies of 6.3 PeV and hence would not be a serious background to multi–W phenomena which are characterized by much higher cascade energies.

For completeness, we have checked the multi–W discovery potential of stage–2 NESTOR subject only to the existence of atmospheric neutrinos or the minimum flux of neutrinos due to protons scattering inelastically off the cosmic microwave background (labelled $z = 0$ in Fig. 2). Only if $\sqrt{\hat{s}_0} \lesssim 3$ TeV and $\hat{\sigma}_0 \gtrsim 10$ μb could stage–2 NESTOR expect to see more than one contained multi–W cascade in 10^7 s due to atmospheric neutrinos. Even less promising is the minimum flux due to the CBR which is at least two orders of magnitude too small to be useful to stage–2 NESTOR in any region of multi–W parameter space.
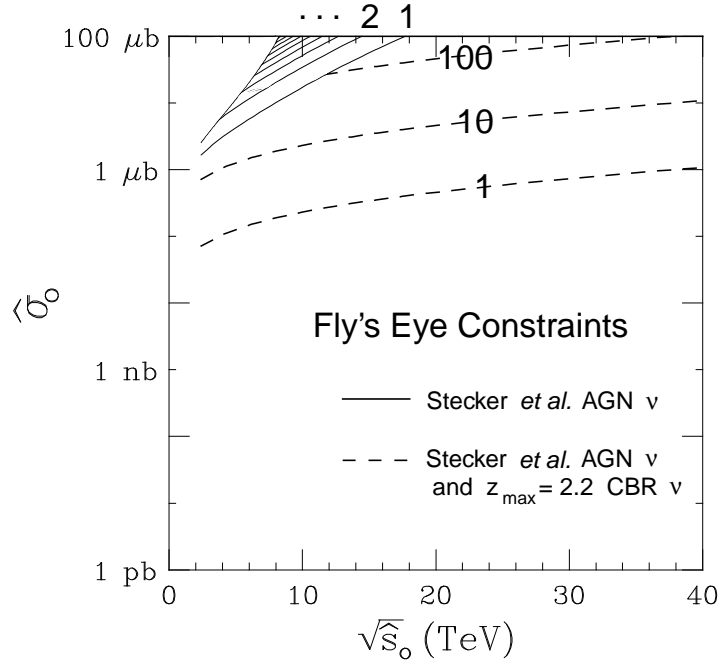

Fig. 10. Number of multi–W events expected by Fly's Eye assuming a) only the Stecker *et al.* AGN neutrino flux (solid contours labelled for 1,2, ... events) and b) sum of the Stecker *et al.* flux and neutrinos produced off the cosmic background radiation (dashed contours).

15

As a final point regarding multi–W processes, we present in Fig. 10 the current best constraints on multi–W phenomena which come from the Fly's Eye experiment (see Ref. 12 for a discussion). Figure 10 supersedes the Fly's Eye constraints presented in Refs. 11, 12; a recent re–evaluation[32] of the Fly's Eye data uncovered an analysis error which overestimated the Fly's Eye's sensitivity to air showers initiated deep in the atmosphere. Consequently, many of the results presented in Ref. 33 (on which we based our earlier constraints) are optimistic by roughly an order of magnitude. Fly's Eye constraints on multi–W phenomena which assume only atmospheric neutrinos or the minimum CBR neutrino flux ($z = 0$ in Fig. 2) are orders of magnitude weaker than those presented in Fig. 10 and hence we do not present them.

3. NESTOR's Sensitivity to Compositeness

3.1. Compositeness Scenarios

The main theoretical reasons for contemplating new physics beyond the Standard Model are well known. The striking generation pattern, *i.e.* the proliferation of quarks and leptons and their deep inter-relations remain mysterious. Composite models of quarks and leptons may offer a scenario for explaining these features[34]. There are a number of composite models based on the hypothesis that (some) leptons and quarks (and possibly even W's and Z's) are bound states of preonic constituents characterized by a compositeness scale (inverse size) Λ_c. However, there is not yet a satisfactory model in which the light masses of quarks and leptons can be reconciled with their small radii $< \mathcal{O}(10^{-16}$ cm$)$ corresponding to a compositeness scale of 1 TeV and beyond. Therefore we will only exploit those features of composite models which are fairly model independent. Reference 35 has explored the features of neutrino-induced air showers in the context of composite models where hypothesized colored subconstituents of PeV neutrinos interact with typical QCD cross sections[36].

3.2. Compositeness Parametrization

Typical features of composite models are new interactions between quarks and leptons and the occurrence of novel particle species such as excited states tow-

ering the known lepton and quark ground states like leptoquarks and leptogluons.

At low energies, $\sqrt{\hat{s}} \ll \Lambda_c$, the new interactions are suppressed by inverse powers of the compositeness scale. The dominant effect should come from the lowest dimensional interactions with four fermions (contact terms) whose most general chirally invariant form reads[37]

$$\frac{\pm g}{2\Lambda^2}\left[\eta_{LL}\overline{\psi}_L\gamma_\mu\psi_L\overline{\psi}_L\gamma^\mu\psi_L + \eta_{RR}\overline{\psi}_R\gamma_\mu\psi_R\overline{\psi}_R\gamma^\mu\psi_R + 2\eta_{LR}\overline{\psi}_L\gamma_\mu\psi_L\overline{\psi}_R\gamma^\mu\psi_R\right]. \tag{5}$$

Such interactions can arise by constituent interchange and/or by exchange of the binding quanta. Various accelerator limits on the scale Λ may be placed through the non–observation[38] of virtual interference effects of the new couplings, Eq. (5), with Standard Model contributions, *e.g.* $\Lambda_{LL}^{+(-)}(eeqq) > 1.7(2.2)$ TeV, $\Lambda_{LL}^{+(-)}(ee\mu\mu) > 4.4(2.1)$ TeV (here we used the conventions of the Review of Particle Properties[38]). The proposed LHC may enlarge such limits to ~ 20 TeV for the compositeness scale probed in quark–quark scattering[39]. At present there are no stringent bounds for neutrino–quark couplings. The *direct* contributions of the new couplings, Eq. (5), to scattering cross sections, being proportional to $\hat{s}/\Lambda^4$, are subdominant when compared to the *virtual* contributions and therefore negligible at present collider energies.

At energies above the compositeness scale ($\sqrt{\hat{s}} \geq \Lambda_c$), the power suppression of the new interactions disappears and a model independent contact interaction analysis ceases to be useful. However, on general grounds one expects[40], in analogy to strong interactions, that the neutrino–quark inelastic cross section saturates, up to logarithmic variations, at a geometrical value set by the compositeness scale,

$$\hat{\sigma}_c(\sqrt{\hat{s}} \geq \Lambda_c) \simeq \frac{\pi}{\Lambda_c^2}, \tag{6}$$

where Λ_c, which characterizes the physical size of the composite neutrinos and quarks, is expected to be related by a factor of $\mathcal{O}(1)$ with the model independent parameters defined in Eq. (5). The final state should be dominated by multi–quark and multi–lepton production.

At neutrino telescopes, the majority of the exotic neutrino–quark scattering processes due to compositeness will come from the center of mass energy region

above the compositeness scale. Correspondingly, we neglect virtual interference effects and direct effects at energies below the compositeness scale which are suppressed by inverse powers of Λ_c. We are thus led to the following simple–minded parametrization of the inelastic cross section of neutrino–quark scattering due to compositeness,

$$\hat{\sigma}_c = \frac{\pi}{\Lambda_c^2} \, \Theta(\sqrt{\hat{s}} - \Lambda_c), \tag{7}$$

which should be sufficient for our purpose. Furthermore we neglect possible $\hat{s}$–channel resonances (leptoquarks). For simplicity, we assume that all quarks and leptons couple with the same strength.

3.3. NESTOR's Compositeness Discovery Potential

Since we have no prediction for prompt multi–muons from composite interactions, we concentrate on detecting contained hadronic and electromagnetic cascades. In Table 1 we present the characteristics of cascades due to compositeness at NESTOR (assuming 10^7s in a 1 km^3 volume) for the Stecker *et al.* AGN neutrino flux and the $z_{\max} = 2.2$ CBR neutrino flux. A quick comparison between the signal and background event rates (with the background rate calculated as in Sect. 2.3) indicates the difficulty of uncovering composite phenomena above $\Lambda_c \gtrsim 1$ TeV. With the same neutrino flux not even the Fly's Eye can place meaningful limits on compositeness due to the small cross sections involved.

Table 1. Characteristics of cascades initiated by neutrino–quark inelastic scattering due to compositeness. The number of cascades refer to 1 km^3 fiducial volume at stage–2 NESTOR in 10^7 s assuming the Stecker *et al.* AGN neutrino flux plus the CBR neutrino flux labelled $z_{\max} = 2.2$ in Fig. 2. Characteristics of background cascades are given in parenthesis.

Λ_c	# of Cascades	$\langle E_{\text{cascade}} \rangle$	$\langle \cos\theta_z \rangle$
1 TeV	120 (360)	120 (3) PeV	.25 (.09)
3 TeV	.4 (140)	1900 (9) PeV	.25 (.10)
5 TeV	.03 (65)	7100 (19) PeV	.33 (.12)

18

4. Leptoquark Searches at NESTOR?

Leptoquarks are color triplet bosons with spin 0 or 1, non–zero lepton and baryon number and fractional electric charge, which couple to lepton–quark pairs. Their appearance is predicted in almost any theoretical scheme beyond the Standard Model which aims at establishing a connection between quarks and leptons, be it by arranging them within common multiplets or by assigning to them common substructure[41]. Clearly, ep colliders such as HERA ($\sqrt{s_{ep}} \simeq 300$ GeV) or LEP–LHC ($\sqrt{s_{ep}} \simeq 1$ TeV) represent ideal machines for hunting leptoquarks[42], since they give rise to dramatic formation peaks in the eq subprocess at a fixed value of $x = m_{LQ}^2/s$.

An exhaustive classification of leptoquarks, whose interactions are B and L conserving, flavor conserving and invariant with respect to the Standard Model transformations and flavor has been performed in Ref. 43. A comprehensive study of indirect bounds on scalar leptoquarks may be found in Ref. 44. The bounds arising from low energy data turn out to be considerably stronger than the first results from the direct searches at HERA[45].

Bergström, Liotta and Rubinstein[14] have discussed the possible effects of scalar leptoquarks at neutrino telescopes. As an example, they considered the production of a scalar leptoquark with weak isospin zero, S_0, whose interactions with the first generation quarks and leptons are given in general by[43]

$$\lambda_L \overline{q}_L^c i\tau_2 \ell_L S_0^\dagger + \lambda_R \overline{u}_R^c e_R S_0^\dagger. \tag{8}$$

According to Eq. (8), the leptoquark S_0 will appear as an $\hat{s}$–channel resonance in the $\nu_e d$ subprocess. Assuming $\lambda_R \equiv 0$[§], S_0 decays into $e + u$ and $\nu_e + d$ in the ratio 1 : 1. As noted in Ref. 14, events of this type may be detected inside large underwater detectors as contained events where the produced electrons will generate multi–TeV cascades ($\langle E_{\text{cascade}} \rangle \sim m_{S_0}^2/2m_p$).

Optimistically assuming a leptoquark mass of 100 GeV[¶], a coupling of the order of the electromagnetic coupling, $\lambda_L = 0.3$, and the "old" Stecker *et al.* AGN neutrino flux (first reference in Ref. 23), Bergström *et al.* predicted about 40 contained downward–moving electron cascades from leptoquarks per year in 2×10^6 t

---

[§]Owing to constraints from pseudoscalar meson decays, leptoquarks with masses of order 100 GeV can have sizeable couplings only to either left– or right–handed leptons[46].

[¶]The direct limit from CDF is $m_{S_0} > 82$ GeV, for $\lambda_R = 0$[47].

in DUMAND II[∥]. This compares to about 20 events from generic $\nu_e N$ charged current interactions. Scaling the leptoquark predictions by $\simeq 1/45$ to account for the revisions to the Stecker *et al.* AGN flux calculation (c.f. second reference in Ref. 23) one would expect 10 contained electron cascades per year in 2.3×10^7 t at stage–2 NESTOR. However, it should be noted that recent indirect bounds give $\lambda_L < 0.03$, for $m_{S_0} = 100$ GeV, $\lambda_R = 0$[44], which reduces the number of electron cascades by another factor of $\sim (.03/.3)^2 = .01$. We thus conclude that the next generation of neutrino telescopes cannot compete with HERA in the search for leptoquarks[42] with masses in the range 100–300 GeV.

5. Conclusions

It is clear that experiments at future supercolliders such as the proton–proton collider LHC and the electron–proton collider LEP–LHC offer the best prospects for observing or constraining exotic phenomena in quark–quark (LHC) and electron–quark (LEP–LHC) scattering in the TeV center of mass range, such as multi–W production, multi–quark and multi–lepton production due to compositeness, and leptoquark production.

Before the era of LHC and LEP–LHC, neutrino telescopes such as AMANDA, Baikal NT–200, DUMAND, and NESTOR suggest alternative strategies to search for exotic scattering phenomena. Neutrino–induced multi–W processes give rise to energetic muon bundles and spectacular multi–PeV cascades. The latter is true also for neutrino–induced multi–hadron and multi–lepton production due to compositeness. Leptoquark production in neutrino–quark scattering generates multi–TeV cascades for leptoquark masses in the hundreds of GeV range. However, the accessible range in parameter space (*i.e.*, the subprocess threshold energy and the size of the subprocess cross section for the multi–W and compositeness scenario, the masses and the couplings of the leptoquarks) depends on the unknown ultrahigh energy neutrino flux.

[∥] The effective volume of DUMAND II for 1 TeV cascades is about 1×10^7 tons[48].

We have found that, within the anticipated parameter range, the prospects to constrain or observe multi–W processes with the help of neutrino telescopes are superior to searches for compositeness and leptoquarks[**]. If a sizeable diffuse flux of ultrahigh neutrinos exists, *e.g.* at the level of the Stecker *et al.* AGN neutrino flux and/or the CBR neutrino flux labelled $z_{\max} = 2.2$ in Fig. 2, neutrino telescopes of the next generation may not only be able to detect it through ordinary charged current interactions, thereby establishing valuable constraints on multi–W parameter space via the Fly's Eye limits, but may even indicate whether multi–W processes are real or an artifact of our imperfect understanding of multi–TeV weak interactions. A sensible search for compositeness and leptoquarks would require even larger neutrino fluxes or detectors larger than stage–2 NESTOR.

6. Acknowledgements

7. References

1. S. Barwick *et al.* (AMANDA Collaboration), in *Proc. 26th Int. Conf. on High Energy Physics*, Dallas, August 1992, ed. J.R. Sanford, (AIP, New York, 1993) Vol. 2, p. 1250.

2. I. Sokalski and Ch. Spiering (eds.) (The Baikal Collaboration), Baikal preprint BAIKAL 92-03 (1992); in *Proc. 23rd Int. Cosmic Ray Conf.*, Calgary, July 1993, ed. D.A. Leaky, (U. of Calgary, 1993), Vol. 4, p. 573; R. Wischnewski, in *these proceedings*.

3. P. Bosetti *et al.* (DUMAND Collaboration), Hawaii DUMAND Center preprint HDC-2-88 (1989); C.M. Alexander *et al.*, in *Proc. 23rd Int. Cos-*

[**]This, however, may be misleading since for multi–W production we parametrized our ignorance by two unrelated parameters, namely the subprocess cross section, $\hat{\sigma}_0$, and the threshold, $\sqrt{\hat{s}_0}$, whereas for the compositeness scenario we had only one parameter, the scale Λ_c, which determines both the subprocess cross section (π/Λ_c^2) and the threshold (Λ_c). A reduction of parameters for multi–W production by assuming that the subprocess cross section above threshold should be given by the geometrical size of the sphaleron $(\hat{\sigma}_0 = \pi/\hat{s}_0)$ or by the S–wave unitarity bound $(\hat{\sigma}_0 = 16\pi/\hat{s})$ would lead to the same poor sensitivity as for compositeness.

mic Ray Conf., Calgary, July 1993, ed. D.A. Leaky, (U. of Calgary, 1993), Vol. 4, p. 515; P. Grieder, in *these proceedings.*

4. L.K. Resvanis (NESTOR Collaboration), in *Proc. Workshop on High Energy Neutrino Astrophysics*, Honolulu, March 1992, eds. V. Stenger, J. Learned, S. Pakvasa and X. Tata, (World Scientific, Singapore, 1993), p. 325; in *these proceedings.*

5. A. Ringwald, *Nucl. Phys.* **B330** (1990) 1.

6. O. Espinosa, *Nucl. Phys.* **B343** (1990) 310.

7. J. Cornwall, *Phys. Lett.* **B243** (1990) 271.

8. H. Goldberg, *Phys. Lett.* **B246** (1990) 445.

9. H. Goldberg, *Phys. Rev.* **D45** (1992) 2945.

10. M. Mattis, *Phys. Rep.* **214** (1992) 159; P. Tinyakov, *Int. J. Mod. Phys.* **A8** (1993) 1823; A. Ringwald, CERN preprint CERN-TH.6862 (1993), to appear in *Proc. 4th Hellenic School on Elementary Particle Physics*, Corfu, Greece, September 1992.

11. D.A. Morris and A. Ringwald in *Proc. 23rd Int. Cosmic Ray Conf.*, Calgary, July 1993, ed. D.A. Leaky, (U. of Calgary, 1993), Vol. 4, p. 407.

12. D.A. Morris and A. Ringwald, CERN preprint CERN-TH.6822 (1993), to appear in *Astropart.Phys.*.

13. D.A Morris and R. Rosenfeld, *Phys. Rev.* **D44** (1991) 3530.

14. L. Bergström, R. Liotta and H. Rubinstein, *Phys. Lett.* **B276** (1992) 231.

15. L. Dell'Agnello *et al.*, INFN Firenze preprint DFF 178/12 (1992), to appear in *Proc. 2nd NESTOR Int. Workshop*, Pylos, October 1992.

16. N. Manton, *Phys. Rev.* **D28** (1983) 2019; Klinkhamer and N. Manton, *Phys. Rev.* **D30** (1984) 2212.

17. V. Zakharov, *Phys. Rev. Lett.* **67** (1991) 3650; *Nucl. Phys.* **B377** (1992) 501; M. Maggiore and M. Shifman, *Nucl. Phys.* **B371** (1992) 177; *ibid.* **B380** (1992) 22; G. Veneziano, *Mod. Phys. Lett.* **A7** (1992) 1661.

18. H. Goldberg, *Phys. Rev. Lett.* **69** (1992) 3017.

19. A. Ringwald and C. Wetterich, *Nucl. Phys.* **B353** (1991) 303; C. Wetterich,

Nucl. Phys. B (Proc. suppl.) **22A** (1991) 43.

20. G. Farrar and R. Meng, *Phys. Rev. Lett.* **65** (1990) 3377.

21. A. Ringwald, F. Schrempp, and C. Wetterich, *Nucl. Phys.* **B365** (1991) 3.

22. L.V. Volkova, *Sov. J. Nucl. Phys.* **31** (1980) 784 [*Yad. Fiz.* **31** (1980) 1510.]

23. F. Stecker, C. Done, M. Salamon, and P. Sommers, *Phys. Rev. Lett.* **66** (1991) 2697; *ibid.* **69** (1992) 2738 (Erratum); in *Proc. Workshop on High Energy Neutrino Astrophysics*, Honolulu, March 1992, eds. V. Stenger, J. Learned, S. Pakvasa and X. Tata, (World Scientific, Singapore, 1993), p. 1.

24. A. Szabo and R. Protheroe, in *Proc. Workshop on High Energy Neutrino Astrophysics*, Honolulu, March 1992, eds. V. Stenger, J. Learned, S. Pakvasa and X. Tata, (World Scientific, Singapore, 1993), p. 24.

25. P. Biermann, in *Proc. Workshop on High Energy Neutrino Astrophysics*, Honolulu, March 1992, eds. V. Stenger, J. Learned, S. Pakvasa and X. Tata, (World Scientific, Singapore, 1993), p. 86; L. Nellen, K. Mannheim, and P. Biermann, *Phys. Rev.* **D47** (1993) 5270.

26. For a review see: T. Stanev, in *these proceedings*.

27. K. Greisen, *Phys. Rev. Lett.* **16** (1966) 748; G. Zatsepin and V.A. Kuzmin, *Pis'ma Zh. Eksp. Teor. Fiz.* **4** (1966) 53 [*JETP Lett.* **4** (1966) 78].

28. V. Berezinskii and G. Zatsepin, in *Proc. 1976 DUMAND Workshop*, Honolulu, September 1976, ed. A. Roberts (Fermilab, Batavia, 1976) p. 15; in *Proc. 15th Int. Cosmic Ray Conf.*, Plovdiv, Bulgaria, August 1977, (Bulgarian Academy of Sciences, Sofia, 1977) p. 248; V. Berezinsky and L. Ozernoy, *Astron. Astrophys.* **98** (1981) 50.

29. F. Stecker, *Astrophys. J.* **228** (1979) 919.

30. C. Hill and D. Schramm, *Phys. Lett.* **B131** (1983) 247; *Phys. Rev.* **D31** (1985) 564.

31. C. Quigg, M.H. Reno and T.P. Walker, *Phys. Rev* **D57** (1986) 774.

32. B. Emerson, Ph.D. thesis, U. of Utah, 1992.

33. R. Baltrusaitis *et al.* (Fly's Eye Collaboration), *Phys. Rev.* **D31** (1985) 2192.

34. For reviews see: H. Harari, *Phys. Rep.* **104** (1984) 159; W. Buchmüller, *Acta Physica Austriaca*, Suppl. **XXVII** (1985) 517.

35. S. Mrenna, *Phys. Rev.* **D45** (1992) 2371.

36. G. Domokos and S. Nussinov, *Phys. Lett.* **B187** (1987) 372; G. Domokos and S. Kovesi–Domokos, *Phys. Rev.* **D38** (1988) 2833.

37. E. Eichten, K. Lane and M. Peskin, *Phys. Rev. Lett.* **50** (1983) 811.

38. K. Hikasa *et al.* (Particle Data Group), *Phys. Rev.* **D45** (1992) IX.12.

39. E. Argyres *et al.*, in *Proc. of the Large Hadron Collider Workshop*, Aachen, Germany, October 1990, eds. G. Jarlskog and D. Rein, (CERN 90–10, ECFA 90–133, Geneva, 1990), Vol. II, p. 805.

40. F. Halzen, K. Hikasa and T. Stanev, *Phys. Rev.* **D34** (1986) 2061.

41. B. Schrempp, in *Proc. Workshop Physics at HERA*, Hamburg, Germany, October 1991, eds. W. Buchmüller and G. Ingelman, (DESY, Hamburg, 1992), Vol. 2, p. 1034.

42. P. Schleper, in *Proc. Workshop Physics at HERA*, Hamburg, Germany, October 1991, eds. W. Buchmüller and G. Ingelman, (DESY, Hamburg, 1992), Vol. 2, p. 1043.

43. W. Buchmüller, R. Rückl and D. Wyler, *Phys. Lett.* **B191** (1987) 442.

44. M. Leurer, Weizmann Institute preprint, WIS–93/90/Sept-PH, hep–ph/9309266, September 1993.

45. M. Derrick *et al.* (ZEUS Collab.), *Phys. Lett.* **B306** (1993) 173; I. Abt *et al.* (H1 Collab.), *Nucl. Phys.* **B396** (1993) 3.

46. W. Buchmüller and D. Wyler, *Phys. Lett.* **B177** (1986) 377.

47. S. Moulding (CDF Collab.), in *Proc. Seventh Meeting of the APS*, Fermilab, USA, November 1992, ed. C. Albright, (World Scientific, Singapore, 1993) 1268.

48. J. Learned, private communication.